MULTI-LOOP CALCULATIONS IN THE STANDARD MODEL: TECHNIQUES AND APPLICATIONS*

J. FLEISCHER, M. TENTYUKOV** AND O.L. VERETIN†

Fakultät für Physik, Universität Bielefeld
D-33615 Bielefeld, Germany
e-mail: fleischer@physik.uni-bielefeld.de
tentukov@thsun1.jinr.dubna.su
veretin@physik.uni-bielefeld.de

(Received October 31, 1997)

We present a review of the Bielefeld-Dubna activities on the multiloop calculations. In the first part a C-program DIANA (DIagram ANAlyser) for the automation of Feynman diagram evaluations is presented, in the second part various techniques for the evaluation of scalar diagrams are described, based on the Taylor expansion method and large mass expansion.

PACS numbers: 12.15. Lk

1. Automation of Feynman diagram evaluation

Recent high precision experiments require, on the side of the theory, high-precision calculations resulting in the evaluation of higher loop diagrams in the Standart Model (SM). For specific processes thousands of multiloop Feynman diagrams do contribute, and it turns out to be impossible to perform these calculations by hand. This makes the request for automation a high-priority task.

Several different packages have been developed with different areas of applicability. For example, FEYNARTS / FEYNCALC [1] are MATHEMATICA packages convenient for various aspects of the calculation of radiative corrections in the SM. There are several FORM packages for evaluating multiloop diagrams, like MINCER [2], and a package [3] for the calculation of

* Presented at the XXI School of Theoretical Physics "Recent Progress in Theory and Phenomenology of Fundamental Interactions", Ustroń, Poland, September 19–24, 1997.

** On leave of absence from Joint Institute for Nuclear Research, 141980 Dubna, Moscow Region, Russian Federation.

† Supported by Bundesministerium für Forschung und Technologie under PH/05-7BI92P 9.

3-loop bubble integrals with a mass. Other automatic packages are GRACE [4] and COMHPEP [5], which partially perform full calculations, from the process definition to the cross-section values.

A somewhat different approach is persued by XLOOPS [6]. A graphical user interface makes XLOOPS an 'easy-to-handle' program package, but is mainly aimed to the evaluation of single diagrams. To deal with thousands of diagrams, it is neccessary to use special techniques like databases and special controlling programs. In [7] for evaluating more than 11000 diagrams the special database-like program MINOS was developed. It calls the relevant FORM programs, waits until they finished, picks up their results and repeats the process without any human interference.

All these packages have different efficiency in different domains. It seems impossible to develop an universal package, which will be effective for all tasks. This point of view motivated us to seek our own way of automatic evaluation of Feynman diagrams.

Our first step is dedicated to the automation of the muons two-loop anomalous magnetic moment (AMM) $\frac{1}{2}(g-2)_\mu$. For this purpose, the package TLAMM was developed [8]. The algorithm is implemented as a FORM-based program package. For generating and automatically evaluating any number of two-loop self-energy diagrams, a special C-program has been written. This program creates the initial FORM-expression for every diagram generated by QGRAF [10], executes the corresponding subroutines and sums up the various contributions. In the SM 1832 two-loop diagrams contribute in this case. The calculation of the bare diagrams is finished. For the purpose of demonstration, we have applied TLAMM to a closed subclass of diagrams of the SM which we refer to as a "toy" model. Some details of the calculation are presented for this case.

A more general project called DIANA (DIagram ANAlyser) [9] for the evaluation of Feynman diagrams is being finished by our group at present and will also be shortly described below.

1.1. The toy model

We considered as a toy example the model involving a light charged spinor Ψ, a photon A_μ, and a heavy neutral scalar field Φ. The scalar has triple (g) and quartic (λ) self-interactions, and the Yukawa coupling (y) to the spinor. The Lagrangian of this model reads (in Euclidean space-time)

$$L = \frac{1}{2}\partial_\mu\Phi\partial^\mu\Phi + \frac{1}{2}M^2\Phi^2 - \frac{g}{3!}\Phi^3 - \frac{\lambda}{4!}\Phi^4 + \frac{1}{4}\left(\partial_\mu A_\nu - \partial_\nu A_\mu\right)^2 + \frac{1}{2\alpha}\left(\partial_\mu A^\mu\right)^2 + \bar{\Psi}\left(\hat{\partial} + ie\hat{A} + m\right)\Psi - y\Phi\bar{\Psi}\Psi\,, \tag{1}$$

where e is the electric charge and α is a gauge fixing parameter.

There are 40 diagrams contributing to the two-loop AMM of the fermion. The calculation of the AMM reduces, after differentiation and contractions with projection operators, to diagrams of the propagator type with external momentum on the fermion mass shell (for details see [11]). After performing the Dirac and Lorentz algebra, all diagrams can be reduced to some set of master integrals.

For the evaluation of these integrals, we use the asymptotic expansion in large masses [12]. For a given scalar graph G, the expansion in large mass is given by the formula

$$F_G(q, M, m, \varepsilon) \overset{M\to\infty}{\sim} \sum_\gamma F_{G/\gamma}(q, m, \varepsilon) \circ T_{q^\gamma, m^\gamma} F_\gamma(q^\gamma, M, m^\gamma, \varepsilon), \quad (2)$$

where γ's are subgraphs involved in the asymptotic expansion, G/γ denotes shrinking of γ to a point; F_γ is the Feynman integral corresponding to γ;

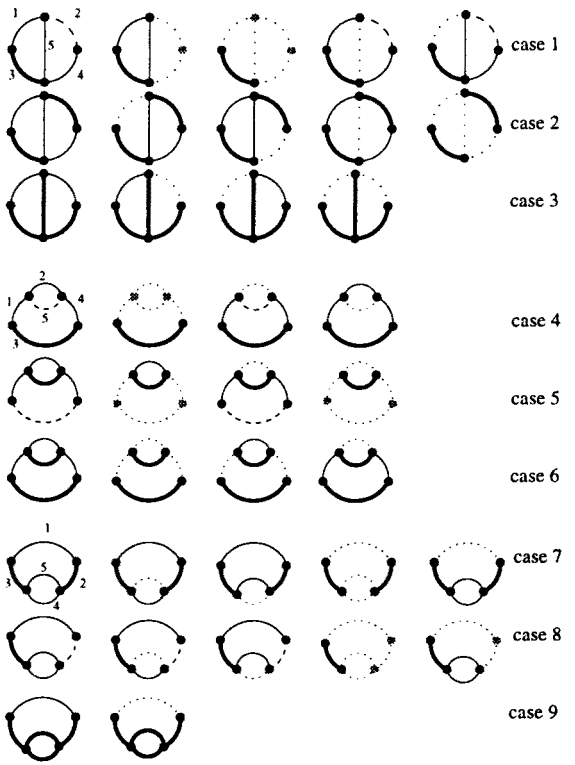

Fig. 1. The prototypes and their subgraphs contributing to the large mass expansion in the toy model. Thick, thin and dashed lines correspond to the heavy-mass, light-mass, and massless propagators, respectively. Dotted lines indicate the lines omitted in the subgraph γ.

T_{q_γ, m_γ} is the Taylor operator expanding the integrand in small masses $\{m_\gamma\}$ and external momenta $\{q_\gamma\}$ of the subgraph γ ; $\circ$ stands for the convolution of the subgraph expansion with the integrand $F_{G/\gamma}$. The sum goes over all subgraphs γ which (a) contain all lines with large masses, and (b) are one-particle irreducible w.r.t. light lines.

Individual integrals are specified by the powers of the scalar denominators, called indices of the lines. From the point of view of the asymptotic expansion method the topology of the diagram is essential. All diagrams of the toy model that contribute to the two-loop AMM can be classified in terms of 9 prototypes (we omit the pure QED diagrams). These prototypes and their corresponding subgraphs involved in the asymptotic expansion, are given in Fig. 1. Almost all integrals occuring in the asymptotic expansion of the muon AMM in the SM can be evaluated analytically using the package SHELL2 [13].

1.2. The piloting C-program TLAMM

For the automatic calculation we have created a special piloting program written in C. This program

1. reads QGRAF output;
2. creates a file containing the complete FORM program for calculating each diagram;
3. executes FORM;
4. reads FORM output, picks out the result of the calculation, and builds the total sum of all diagrams in a single file which can be processed by FORM.

Identifiers for vertices and propagators and the explicit Feynman rules are read from separate files and then inserted into the FORM program. Because the number of identifiers needed for the calculation of all diagrams at once may exceed the FORM capacity, the piloting program retains for each diagram only those involved in its calculation.

All initial settings are defined in a configuration file. The latter contains information about the file names, identifiers of topologies, the distribution of momenta, and the description of the model in terms of the notation that is some extension of QGRAF's. The program carries out the complete syntax check of all input files except the QGRAF output.

There exist several options which allow one to process only the diagrams

- explicitly listed by number;
- of a given prototype;
- of a specified topology.

There are also some debugging options.

QGRAF generates the diagrams in symbolic form in terms of vertices. Fig. 2 shows one of the diagrams in the toy model with the corresponding QGRAF output.

```
. . .
*--#[ d2:
*
     1
    *vx(E2(2),e2(-1),H(1))
    *vx(E2(3),e2(4),A(-3))
    *vx(E2(-2),e2(5),H(6))
    *vx(E2(5),e2(3),H(1))
    *vx(E2(4),e2(2),H(6))
*
*--#] d2:
. . .
```

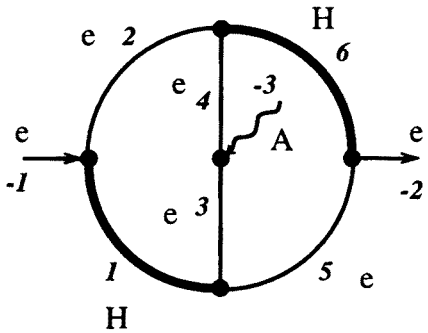

Fig. 2. Diagram "number 2". `e2` stands for fermion, `E2` for anti-fermion, `H` is a scalar, and `A` the photon. External legs are numbered by negative numbers and vx stands for the vertex for the particles in the argument list.

The Feynman integrand generated by the C-program for this diagram reads:

```
g VF(mu)=
E2_H_e2*F_F(-k2+p,q/2,me2)*E2_H_e2*F_F(k1-k2,q/2,me2)*
A_E_e(mu)*F_F(k1-k2,-q/2,me2)*E2_H_e2*F_F(k1,-q/2,me2)*
E2_H_e2*H_H(k1-p,0)*H_H(k2,0);                          (3)
```

A demo diskette for evaluating the toy model can be provided on request.

1.3. Project DIANA

At present we have finished the main part of the more general program DIANA (DIagram ANAlyser). For generating Feynman diagrams we use again QGRAF. The program DIANA consists of two parts:

- Analyzer of diagrams.
- Interpreter of a special text manipulating language (TM);

The TM language is a very simple TeX-like language for creating source code and organizing the interactive dialog.

The analyzer reads QGRAF output and passes necessary information to the interpreter. For each diagram the interpreter performs the TM-program,

producing input for further evaluation of the diagram like for example (3). Thus the program:

Reads QGRAF output and for each diagram it:

1. Defines the topology.
2. Looking for it in the table of all known topologies and distributes momenta according to the current topology.
3. Creates a special internal representation of the diagram corresponding to the Feynman integrand.
4. Invokes the interpreter to execute the TM-program and passes to it the necessary data.

Executing the TM-program provides the possibility to calculate each diagram using FORM or another formulae manipulating language, to do some numerical calculation by means of FORTRAN, to create a postscript file for the picture of the current diagram, *etc.*

If we do not yet know all needed topologies, we may use the program to determine missing topologies that occur in the process.

The main goal of the TM-language is the creation of text files. In principle, we could have used one of the existing languages, but we want a very specific language: it should be powerful enough to create arbitrary program texts. On the other hand, it should be very simple and easy-in-use, so that even non-programmers can use it.

Similar to the TeX language, all lines without special escape-characters ("\") are simply typed to the output file. So, to type "Hello, world!" in the file "hello" we may write down the following program:

```
\program
\setout(hello)
Hello, world!
```

Each word whose first character is an escape character will be considered as a command. This feature makes this language very easy-to-use.

At present we have finished the C-part of this project.

2. Evaluation of scalar diagrams

In this part, methods for the evaluation of scalar three point functions will be discussed. We will concern ourselves with the Taylor expansion with respect to an external momentum squared and the large mass expansion explained above. The efficiency of both approaches will be compared.

2.1. Expansion of three-point functions in terms of external momenta squared

Taylor series expansions in terms of one external momentum squared, q^2 say, were considered in [14], Padé approximants were introduced in [15] and in Ref. [16] it was demonstrated that this approach can be used to calculate Feynman diagrams on their cut by analytic continuation. The Taylor coefficients are expressed in terms of "bubble diagrams", *i.e.* diagrams with external momenta equal zero, which makes their evaluation relatively easy. In the case under consideration, we have two independent external momenta in $d = 4 - 2\varepsilon$ dimensions. The general expansion of (any loop) scalar 3-point function with its momentum space representation $C(p_1, p_2)$ can be written as

$$C(p_1, p_2) = \sum_{l,m,n=0}^{\infty} a_{lmn} (p_1^2)^l (p_2^2)^m (p_1 p_2)^n , \tag{4}$$

where the coefficients a_{lmn} are to be determined from the given diagram.

For many applications, it suffices to confine to the case $p_1^2 = p_2^2 = 0$, which is *e.g.* physically realized in the case of the Higgs decay into two photons ($H \to \gamma\gamma$) with p_1 and p_2 the momenta of the photons. In this case, only the coefficients a_{00n} are needed.

In the two-loop case we consider the scalar integral ($k_3 = k_1 - k_2$, see also Fig. 3)

$$C(m_1, \cdots, m_6; p_1, p_2) = \frac{1}{(i\pi^2)^2} \times \int \frac{d^4k_1 d^4k_2}{((k_1+p_1)^2-m_1^2)((k_1+p_2)^2-m_2^2)((k_2+p_1)^2-m_3^2)((k_t+p_2)^2-m_4^2)(k_2^2-m_5^2)(k_3^2-m_6^2)} . \tag{5}$$

k_t in line 4 (with mass m_4) depends on the topology: for the *planar* diagram we have $k_t = k_2$ while for the *non-planar* we have $k_t = k_3$.

With obvious abbreviations for the scalar propagators: c_i the i^{th} scalar propagator of (5) with $p_1 = p_2 = 0$, we can quite generally write for the n^{th} Taylor coefficient [18]:

$$(i\pi^2)^2 a_{00n} = \frac{2^n}{n+1} \int d^4k_1 d^4k_2 F_n \frac{1}{c_1\ c_2\ c_3\ c_4\ c_5\ c_6} . \tag{6}$$

The numerator F_n can be written as

$$F_n = \sum_{\nu=0}^{n} c_1^{-(n-\nu)} c_3^{-\nu} \sum_{\nu'=0}^{n} c_2^{-(n-\nu')} c_4^{-\nu'} A^n_{\nu\nu'}(k_1, k_2, k_t) \tag{7}$$

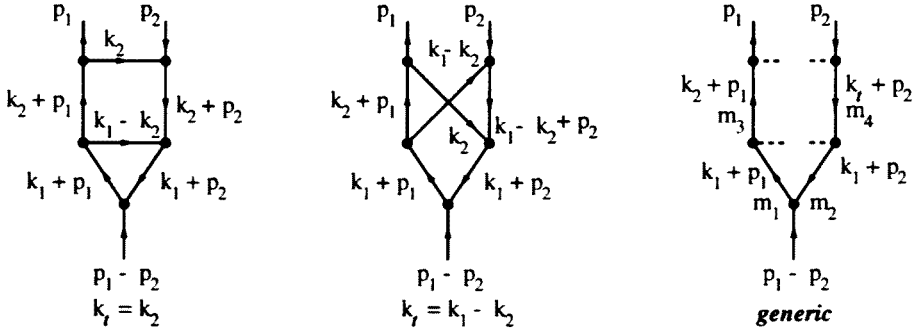

Fig. 3. Planar and non-planar scalar vertex diagrams and their kinematics

with

$$A^n_{\nu\nu'}(k_1,k_2,k_t) = \sum_{\mu=0}^{\left[\frac{\nu+\nu'}{2}\right]} \sum_{\sigma=0}^{\left[\frac{\nu}{2}\right]} \sum_{\tau=0}^{\left[\frac{\nu'}{2}\right]} b^{n\mu,\sigma\tau}_{\nu\nu'}$$
$$\times (k_1^2)^{n-(\nu+\nu')+\mu} (k_2^2)^{\sigma} (k_1k_2)^{\nu-\mu-\sigma+\tau} (k_1k_t)^{\nu'-\mu+\sigma-\tau} (k_2k_t)^{\mu-\sigma-\tau} (k_t^2)^{\tau}, \quad (8)$$

where the coefficients $b^{n\mu,\sigma\tau}_{\nu\nu'}$ are given by

$$b^{n\mu,\sigma\tau}_{\nu\nu'} = (n+1)\ 2^{\lambda-n-1}\ (n-\nu)!\ (n-\nu')!\nu!\ \nu'! \frac{\Gamma(d-1)}{\Gamma(n+d-2)\Gamma(n+\frac{d}{2})}$$
$$\times \frac{2^{2\rho}}{\rho!\sigma!\tau!} \sum_{i=1}^{[\frac{n}{2}]+1} (-4)^{i-1}(i-1)!\ \Gamma(n+\frac{d}{2}-i)$$
$$\times \sum_{j=\max(0,n_i-\nu)}^{\min(n_i,n-\nu)} \sum_{k=\max(0,n_i-\nu')}^{\min(n_i,n-\nu')} \frac{2^{j+k}}{(n_i-j-\rho)!(n_i-k-\rho)!(\rho+j+k-n_i)!}$$
$$\times \frac{1}{\sigma_j!(\nu_j-2\sigma)!\tau_k!(\nu'_k-2\tau)!}, \quad (9)$$

with $\lambda = \nu+\nu'-2\mu$, $\rho = \mu-\sigma-\tau$, $\nu_j = \nu-n_i+j$, $\nu'_k = \nu'-n_i+k$, $\sigma_j = \sigma-[j-(n-\nu)+(i-1)]$ and $\tau_k = \tau-[k-(n-\nu')+(i-1)]$.

For the *planar* diagram ($k_t = k_2$) (8) simplifies and we have

$$A^n_{\nu\nu'}(k_1,k_2) = \sum_{\mu=\max(0,\nu+\nu'-n)}^{\left[\frac{\nu+\nu'}{2}\right]} a^{n\mu}_{\nu\nu'} (k_1^2)^{n-(\nu+\nu')+\mu} (k_2^2)^{\mu} (k_1\ k_2)^{\nu+\nu'-2\mu}, \quad (10)$$

with

$$a^{n\mu}_{\nu\nu'} = \sum_{\sigma=0}^{\left[\frac{\mu}{2}\right]} \sum_{\tau=0}^{\left[\frac{\nu'}{2}\right]} b^{n\mu,\sigma\tau}_{\nu\nu'} \,. \tag{11}$$

The coefficients $a^{n\mu}_{\nu\nu'}$ are mass independent and have been calculated with FORM up to order ε^2 ($d = 4 - 2\varepsilon$) and stored for the first 30 Taylor coefficients, *i.e.* they are given in terms of rational numbers. For the *non-planar* case the situation is more difficult since the storing of the coefficients $b^{n\mu,\sigma\tau}_{\nu\nu'}$ with two more indices is practically impossible for high Taylor coefficients. In many cases, however, if the threshold of the diagram under consideration is high, only a few (say 8) Taylor coefficients are sufficient for a high precision calculation of the diagram under consideration and in such a case the direct calculation of the $b's$ in each case causes no problem.

Finally all remaining integrals can be reduced to bubble-integrals of the type

$$V_{\alpha\beta\gamma}(\{m\}) = \int \frac{d^d k_1 d^d k_2}{(k_1^2 - m_1^2)^\alpha (k_2^2 - m_2^2)^\beta ((k_1 - k_2)^2 - m_3^2)^\gamma}, \tag{12}$$

or to factorizing one-loop integrals.The genuine two-loop bubble integrals are reduced by means of recurrence relations to $V_{111}(\{m\})$. This can be done numerically for the arbitrary mass case or also analytically for special cases like *e.g.* only one non-zero mass. For details see [17, 18]. To perform the recursion numerically, it is important to use the multiple precision FORTRAN by D. Bailey ([19]) since tremendeous cancellations occur in this case.

We have in some detail presented one approach for the calculation of the Taylor expansion of Feynman diagrams, others were worked out in Refs. [20, 21]. The latter one is particularly suited for programming in terms of a formulae manipulating language like FORM.

2.2. The method of analytic continuation

Assume, the following Taylor expansion of a scalar diagram or a particular amplitude is given $C(p_1, p_2, \ldots) = \sum_{m=0}^{\infty} a_m y^m \equiv f(y)$ and the function on the r.h.s. has a cut for $y \geq y_0$. In the above case of $H \to \gamma\gamma$ one introduces $y = q^2/4m_t^2$ with $q^2 = (p_1 - p_2)^2$ as adequate variable with $y_0 = 1$.

The method of evaluation of the original series consists in a first step in a conformal mapping of the cut plane into the unit circle and secondly the reexpansion of the function under consideration into a power series w.r.t. the new conformal variable

$$\omega = \frac{1 - \sqrt{1 - y/y_0}}{1 + \sqrt{1 - y/y_0}} \,. \tag{13}$$

By this conformal transformation, the y-plane, cut from y_0 to $+\infty$, is mapped into the unit circle (see Fig. 4) and the cut itself is mapped on its boundary, the upper semicircle corresponding to the upper side of the cut. The origin goes into the point $\omega = 0$.

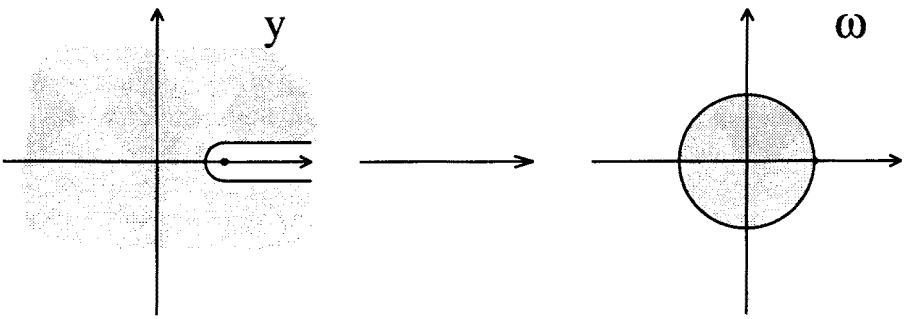

Fig. 4. Conformal mapping of the $y = q^2/4m_t^2$-complex plane into the ω-plane.

After conformal transformation it is suggestive to improve the convergence of the new series w.r.t. ω by applying the Padé method [22, 23]. A convenient technique for the evaluation of Padé approximations is the ε-algorithm of [22] which allows one to evaluate the Padé approximants recurrsively.

Historically the first example considered was the two-loop three-point scalar (*planar*) integral with the kinematics of the decay $H \to \gamma\gamma$: $m_6 = 0$ and all other masses $m_i = m_t (i = 1, \ldots, 5)$. In this special case all Taylor coefficients can be expressed in terms of Γ-functions. Later a closed expression for arbitrary coefficients has been found in [21].

Results for this kinematics on the cut are given in Table I. The process $H \to \gamma\gamma$ was investigated before in Ref. [24]. For the master integral under consideration in [24], all integrations but one could be performed analytically and only the last one had to be done numerically. Similarly, high precision is obtained on the cut in the approach of [16].

Further examples of the efficiency of our method were given in Refs. [25] and [26]. In the latter case a diagram of particular interest for the $Z \to b\bar{b}$ decay has been considered, namely a planar diagram with a low threshold: $m_1 = m_2 = m_5 = m_6 = m_b = 4.5$ GeV and $m_3 = m_4 = m_Z = 91$ GeV. If this diagram is to be evaluated on the Z mass-shell, a precision of only some four decimals can be obtained with 30 Taylor coefficients, which is hardly good enough. On the other hand it is a very reasonable approximation in this case to put $m_b = 0$ from the very beginning and thus consider diagrams with zero thresholds, which should be evaluated more easily with higher precision. These will be considered in the next section.

TABLE I

Results on the cut ($q^2 > 4m_t^2$) in comparison with [24]

q^2/m_t^2	[14/14]		Ref. [24]	
	Re	Im	Re	Im
4.01	11.935	12.699	11.9347(1)	12.69675(8)
4.10	2.66245	9.0955	2.66246(2)	9.0954(2)
5.0	−1.985804823	2.758626375	−1.98580(2)	2.758625(2)
10.0	−0.7569432708	−0.0615483234	−0.756943(1)	−0.061547(1)
40.0	−0.045852780	−0.0645672604	−0.04585286(7)	−0.0645673(9)
400.0	+0.00008190	−0.0021670	0.0000818974(3)	−0.002167005(3)

2.3. Two-loop vertex diagrams with zero thresholds

Concerning the vertex diagrams, there are many different topologies contributing to a 3-point function in the SM. For our purpose of demonstrating the method, we confine ourselves to the planar case shown in Fig. 5a. Figs. 5c, d present infrared divergent diagrams.

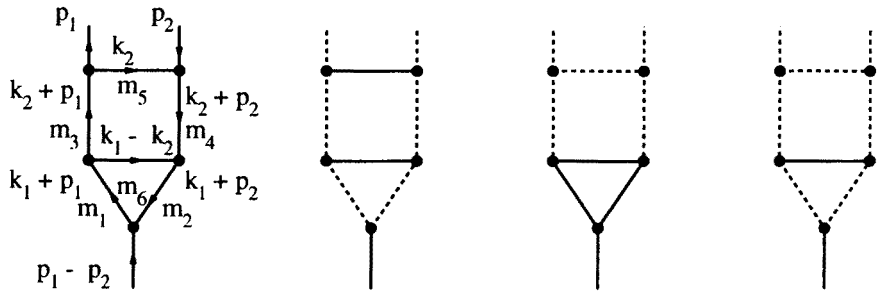

Fig. 5. Planar diagrams with zero thresholds. a—generic; b—IR finite diagram; c, d—IR divergent diagrams.

As a typical (and very complicated case) we consider here Fig. 5b with equal non-zero masses [27]. There are two massless cuts so that we shall have the double logarithm in the expansion. The set of subgraphs in this case is given by $\gamma_1 = \Gamma$ and the higher terms with $\gamma \neq \Gamma$: $\gamma_2 = \{3456\}$, $\gamma_3 = \{1256\}$, and $\gamma_4 = \{56\}$ (in curly brackets: the line numbers of the subgraphs γ in (2), line numbers are shown in Fig. 5). Note that γ_3 and γ_4 are disconnected. After summing up all four contributions we see that the double and single poles in ε cancel as well as the scale parameter μ, with

the result ($x = q^2/M^2$)

$$F_\Gamma(q^2, M^2) = \frac{1}{M^4} \sum_{n=0}^{\infty} \sum_{j=0}^{2} f_{jn} \ln^j(-x) x^n$$
$$\equiv \frac{1}{M^4} \left\{ f_0(x) + f_1(x) \ln(-x) + f_2(x) \ln^2(-x) \right\}, \quad (14)$$

where the f_{jn} are now given in terms of rational numbers and $\zeta(2)$. $f_2(x)$ can be summed analytically, yielding

$$f_2(x) = (\ln|1+x| - i\pi\theta(1+x))^2/x^2. \quad (15)$$

Thus, we have to Padé approximate f_0 and f_1 only. Close to the second threshold at $q^2 = M^2$ the convergence is indeed excellent (see Table II) [27]. It should be noted that for the physical application we have in mind, *i.e.* $Z \to b\bar{b}$, this is just the case of interest. It is worthwhile to note the sharp increase for low q^2 due to $\ln^2(-q^2/M^2)$.

TABLE II

Results for timelike q^2 for diagram 5b

q^2/M^2	[12/12]		Ref. [24]	
	Re	Im	Re	Im
0.05	+2.948516245	20.938528	+2.948516245	20.938528
0.1	−1.108116127	16.04132127	−1.108116127	16.04132127
0.5	−4.820692281	5.066080015	−4.820692281	5.066080015
1.0	−3.890154	1.67549787	−3.890156	1.67549788
1.5	−2.904588	0.42979	−2.904581	0.429778
2.0	−2.18294	−0.06976	−2.182981	−0.069728
10.0	−0.191	−0.208	−0.194	−0.215

Infrared divergent diagrams (Figs. 5c,d have been successfully considered in [28]. For Fig. 5c the convergence is indeed excellent again. The different mass case, *i.e.* $m_6 \neq m_1 = m_2$, had to be calculated numerically according to the procedure outlined in Sect. 2.1. For Fig. 5d, the convergence is by far not that good: for $q^2/M^2 = 1$, a precision of 6 decimals is still obtained with a [15/15] approximant, while for $q^2/M^2 \simeq 10$ only 2 decimals were obtained (see Table III) where the "numerical results" were obtained by the method of Ref. [29].

TABLE III

The finite part for diagram 5d

q^2/m_6^2	[15/15]		numerical results	
	Re	Im	Re	Im
0.5	81.17501719	12.06458720	81.1750	12.0644
1.0	17.7659	19.97799834	17.7658	19.9779
2.0	− 0.6047	7.3759	− 0.604	7.376
10.0	− 0.572	0.023	− 0.570	0.025

This much slower convergence implies that indeed it is very desirable to have, at least in the case of only one non-zero mass, a compact representation of the Taylor coefficients in terms of rational numbers, *i.e.* not to have to go through the mashinery of calculating the coefficients as described in Sect. 2.1. Such a possibility will be described in the next section.

2.4. The differential equation method

We saw that to obtain the expansion of a diagram one has to go through a rather combersome machinery. The more coefficients are asked for, the more efforts and machine resourses are required. Thus it is very desirable to have analytic expressions for expansion coefficients whenever possible. This can be done with the aid of the Differential Equation Method (DEM) [30] if only one non-zero mass occurs. The DEM allows one to get results for massive diagrams by reducing the problem to diagrams with simpler structure.

Let us introduce a graphical notation for the scalar propagators (in euclidean space-time)

$$\frac{1}{(q^2)^\alpha} = \overset{\alpha}{\bullet\!\cdots\!\bullet} \,, \qquad \frac{1}{(q^2+m^2)^\alpha} = \overset{\alpha}{\underset{m^2}{\bullet\!-\!\bullet}}$$

α and m refer to the index and mass of a line. Then one can derive the following recurrence relation for a massive triangle [30]

$$\overset{\alpha_2}{\underset{\alpha_1}{\triangle}}{}^{\alpha_3} (D - 2\alpha_1 - \alpha_2 - \alpha_3) = -2m_1^2\alpha_1 \overset{\alpha_2}{\underset{\alpha_1+1}{\triangle}}{}^{\alpha_3}$$

$$+\alpha_2\left(\overset{\alpha_2+1}{\underset{\alpha_1-1}{\triangle}}{}^{\alpha_3} - \overset{\alpha_2+1}{\underset{-1\quad\alpha_1}{\triangle}}{}^{\alpha_3} - (m_1^2+m_2^2)\overset{\alpha_2+1}{\underset{\alpha_1}{\triangle}}{}^{\alpha_3}\right) + (\alpha_2 \leftrightarrow \alpha_3)$$

along with some other graphical relations (see details in [30]).

Using this technique we analysed in [31] the class of 3-point two-loop massive graphs. As an example for the diagram of Fig. 5c we get

$$(D-4)J_{5c} = 2$$ 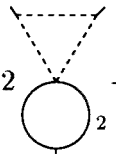 $$- 2$$ 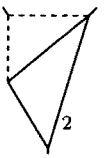 $$- 4m^2$$ 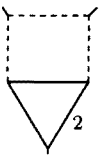 $$- 2m^2$$ 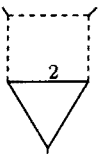 (16)

In the r.h.s. of (16), the last two terms can be combined, resulting in $\mathrm{d}J/\mathrm{d}m^2$ while for the second term we proceed in turn as

$$(D-4)$$ 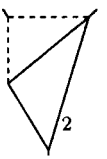 $$=$$ 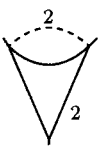 $$+$$ 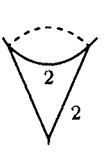 $$-$$ 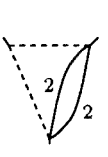 (17)

Thus we are left with simple diagrams (these can be done completely by Feynman parameters) and the derivative of the initial diagram w.r.t. m^2. The solution of the corresponding differential equation in terms of a series obtained from an integral representation reads

$$J_{5c} = -\frac{\Gamma^2(1+\mathrm{e})}{(q^2)^2(m^2)^{2\mathrm{e}}}\sum_{n=1}^{\infty}\frac{(-x)^n\Gamma^2(n)}{\Gamma(2n+1)}\left[\frac{1}{\mathrm{e}^2} - \frac{1}{\mathrm{e}}\Big(\ln(x)+S_1(n-1)\Big) - \frac{3}{2}S_2(n-1)\right.$$
$$\left. - \frac{15}{2}S_1^2(n-1) + 4S_1(n-1)S_1(2n) - \zeta(2) - \ln(x)S_1(n-1) + \frac{1}{2}\ln^2(x)\right],$$

where

$$S_l(n) = \sum_1^n \frac{1}{k^l}\,.$$

A similar formula was obtained for the diagram of Fig. 5 d (see [31]).

2.5. Large mass expansion versus small momentum expansion

If there are two or more different masses involved the coefficients a_{lmn} in (4) are not just numbers any more but complicated functions of mass ratios. In this case one can try to perform a large mass (LM) expansion rather than a small momentum expansion.

Here we just consider one example of a large mass expansion for the 3-point function (a more detailed analysis will be given in [32]). Let us consider the diagram of Fig. 6a with two non-zero masses m_W and m_{top}, contributing to Z decay in the SM. Thus we have $q^2 = m_Z^2$. One can use

the procedure described in Sect. 2.1 to expand this diagram in the external momentum squared. Then the actual parameter of expansion is $q^2/m_{\rm top}^2$ and the radius of convergence is given by the lowest (non-zero) threshold *i.e.* $q^2 = (m_{\rm top} + m_W)^2 \gg m_Z^2$. Another possibility is to expand in the ratios $q^2/m_{\rm top}^2$ and $m_W^2/m_{\rm top}^2$, though one will see that this expansion does not work that well.

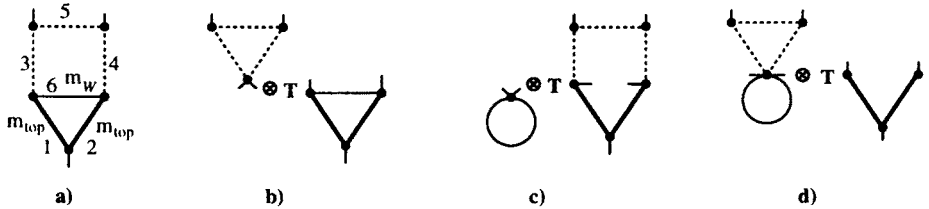

Fig. 6. A planar diagram a with two different masses and subgraphs b, c and d contributing to the large mass expansion series. Dashed lines are massless; solid lines have light mass m_W; bold lines have heavy mass $m_{\rm top}$. T stands for the Taylor expansion w.r.t. external momenta and light mass.

The asymptotic expansion in the limit of the large mass is given by (2). In our case there are 4 subgraphs that contribute, *i.e.* $\gamma_1 = \{123456\}$, $\gamma_2 = \{126\}$, $\gamma_3 = \{12345\}$ and $\gamma_4 = \{12\}$ (see Fig. 6a-d). By direct evaluation we find that there are induced poles of the order $1/\varepsilon^3$ in subgraphs while in the the sum they cancel which serves as a good check. For this particular diagram, the result of the LM expansion looks like

$$\text{dia} = \sum_{n=-1}^{\infty} A_n = \left(b_n^{(0)} + b_n^{(1)} L + b_n^{(2)} L^2 + b_n^{(3)} L^3\right) \left(\frac{1}{m_{\rm top}^2}\right)^n \qquad (16)$$

with $L = \log(m_{\rm top}^2/\mu^2)$ and $b_n^{(i)}$'s being known functions of q^2, m_W^2 and μ^2.

In Table IV we give the results of the numerical analysis for the graph at hand. We observed bad behavior of the series (16): namely 10 coefficients give only 3 stable figures. Since the parameters of expansion $q^2/m_{\rm top}^2$ and $m_W^2/m_{\rm top}^2$ both are of order 0.25 one would expect better convergence. We have found that this bad convergence remains true for some other graphs of the $Zb\bar{b}$ process [32]. Moreover no analytic properties are known in the $1/m^2$ variable and thus no conformal mapping like (13) is now available to improve the convergence. However we apply the Padé summation. Nevertheless the LM expansion for 3-point functions in such a regime looks very attractive since it can be rather easily implemented in formulae manipulating languages like FORM even in the presence of more than one non-zero mass. In the worst case one achives 0.1% accuracy with 10 coefficients. Our programs allow us to get 15-20 coefficients in a reasonable time.

TABLE IV

Terms in the LM expansion corresponding to formula (16) at $\mu = m_{\rm top} = 180$, $m_W = 80, q^2 = 90^2$. The last two lines give Padé approximants obtained with 10 terms of the LM expansion and 8 Taylor coefficients of the small q^2 expansion.

n	Re A_n	Im A_n
−1	−6.35040	+ 29.98705
0	−3.85690	− 6.19256
1	−1.74681	− 4.34057
2	0.22329	− 1.30291
3	0.65892	− 0.21984
4	0.47058	+ 0.00121
5	0.25376	+ 0.01435
6	0.13099	+ 0.00492
7	0.07311	+ 0.00073
8	0.04517	− 0.00009
9	0.02984	− 0.00009
10	0.02042	− 0.00002
LM	−9.996	17.9527
small-q	−9.9926682590236	17.95215366130182

2.6. Conclusion

Any involved calculation in field theory nessesarily consists of two parts: 1 — automatic generation of Feynman diagrams and source codes and 2 — techniques of evaluating scalar Feynman diagrams. In this paper we presented both. Still some efforts have to be applied to handle the numerators of diagrams. We are working also on the automation of the renormalization procedure.

We would like to thank M. Kalmykov for helpful discussion. M. T. and O. V. aknowledge the University of Bielefeld for the warm hospitality.

REFERENCES

[1] J. Küblbeck, M. Böhm, A. Denner, *Comput. Phys. Commun.* **60**, 165 (1990); R. Mertig, M. Böhm, A. Denner, *Comput. Phys. Commun.* **64**, 345 (1991).
[2] S.A. Larin, F.V. Tkachov, J.A.M. Vermaseren, NIKHEF-H/91-18.
[3] L.V. Avdeev, *Comput. Phys. Commun.* **98**, 15 (1996).

[4] T. Ishikawa *et al.*, Minami-Taeya group "GRACE manual", KEK-92-19, 1993.

[5] E.E. Boos *et al.*, SNUTP 94-116 (1994); (hep-ph/9503280).

[6] L. Brücher *et al.*, *Nucl. Instrum. Methods* **A389**, 323 (1997); A. Frink, J.G. Körner, J.B. Tausk, (hep-ph/9709490).

[7] T. van Ritbergen *et al.*, *Int. J. Mod. Phys.* **C6**, 513 (1995).

[8] L.V. Avdeev, J. Fleischer, M. Yu. Kalmykov, M. Tentyukov, *Nucl. Instrum. Methods* **A389**, 343 (1997); *Towards Automatic Analytic Evaluation of Diagrams with Masses*, accepted for publication in *Comput. Phys. Commun.*, (hep-ph/9710222); L.V. Avdeev, M.Yu. Kalmykov, *Nucl. Phys.* **B502**, 419 (1997).

[9] J. Fleischer, M. Tentyukov, "A Feynman Diagram Analyser DIANA", Bielefeld preprint BI-TP-97/44, in preparation.

[10] P. Nogueira, *J. Comput. Phys.* **105**, 279 (1993).

[11] R. Roskies, E. Remiddi, M.J. Levine, in *Quantum Electrodynamics*, ed. T. Kinoshita, World Scientific, Singapore, 1990, p.163.

[12] F.V. Tkachov, Preprint INR P-0332, Moscow (1983); P-0358, Moscow (1984); K.G. Chetyrkin, *Teor. Math. Phys.* **75**, 26 (1988); *Teor. Math. Phys.* **76**, 207 (1988); Preprint, MPI-PAE/PTh-13/91, Munich (1991); V.A. Smirnov, *Commun. Math. Phys.* **134**, 109 (1990); *Renormalization and Asymptotic Expansions*, Birkhäuser, Basel 1991.

[13] J. Fleischer, O.V. Tarasov, *Comput. Phys. Commun.* **71**, 193 (1992).

[14] A.I. Davydychev, J.B. Tausk, *Nucl. Phys.* **B397**, 123 (1993).

[15] D.J. Broadhurst, J. Fleischer, O.V. Tarasov, *Z. Phys.* **C60**, 287 (1993).

[16] J. Fleischer, O.V. Tarasov, *Z. Phys.* **C64**, 413 (1994).

[17] K.G. Chetyrkin, F.V. Tkachov, *Nucl. Phys.* **B192**, 159 (1981); F.V. Tkachov, *Phys. Lett.* **100B**, 65 (1981).

[18] J. Fleischer, O.V. Tarasov, in "Computer Algebra in Science and Engineering", ed. J. Fleischer *et al.*, Bielefeld, 28-31 August 1994, World Scientific, Singapore 1995, p.212.

[19] D.H. Bailey, *ACM Trans. Math. Software* **19**, 288 (1993).

[20] A.I. Davydychev, J.B. Tausk, *Nucl. Phys.* **B465**, 507 (1996).

[21] O.V. Tarasov, *Nucl. Phys.* **B480**, 397 (1996).

[22] D. Shanks, *J. Math. Phys.* **34**, 1 (1955); P. Wynn, *Math. Comput.* **15**, 151 (1961); G.A. Baker, P. Graves-Morris, *Padé Approximants*, in *Encyl. of Math. and its Appl.*, Vol. 13, 14, Addison-Wesley, 1981.

[23] G.A. Baker Jr., J.L. Gammel, J.G. Wills, *J. Math. Anal. Appl.* **2**, 405 (1961); G.A. Baker Jr., Essentials of Padé Approximants, Academic Press, 1975.

[24] A. Djouadi, M. Spira, P.M. Zerwas, *Phys. Lett.* **B311**, 255 (1993).

[25] J. Fleischer, in *Artificial Intelligence and Expert System for High Energy and Nuclear Physics*, ed. B. Denby and D. Perret-Gallix, Pisa, Italy, April 3-8, 1995, p.103.

[26] J. Fleischer, O.V. Tarasov, in *QCD and QED in Higher Orders*, ed. T. Riemann and J. Blümlein, Rheinsberg, Germany, April 21-26, 1996, p.295.

[27] J. Fleischer, V. Smirnov, O.V. Tarasov, *Z. Phys.* **C74**, 379 (1997).

[28] J. Fleischer *et al.*, to be published in *Z. Phys.* **C**, (hep-ph/9704353).

[29] D. Kreimer, *Phys. Lett.* **B273**, 277 (1991).

[30] A.V. Kotikov, *Phys. Lett.* **B254**, 185 (1991); *Phys. Lett.* **B259**, 314 (1991); *Phys. Lett.* **B267**, 123 (1991).

[31] J. Fleischer, A.V. Kotikov, O.L. Veretin, Bielefeld preprint BI-TP-97/26, *Phys. Lett.* in print, (hep-ph/9707492).

[32] J. Fleischer, M. Kalmykov, O. Veretin, Large Mass Expansion versus Small Momentum Expansion of Feynman Diagrams, Bielefeld preprint BI-TP-97/43, in preparation.